Contents lists available at ScienceDirect

Comptes Rendus Chimie

www.sciencedirect.com

Full paper/Mémoire

Heterogeneous Fenton-like reactions with a novel hybrid Cu−Mn−O catalyst for the degradation of benzophenone-3 in aqueous media

Zhang Zhang [a], Yang Guo [a], Qiang Wang [a, *], Benoît Louis [b], Fei Qi [a, **]

[a] Beijing Key Lab for Source Control Technology of Water Pollution, College of Environmental Science and Engineering, Beijing Forestry University, 35 Qinghua East Road, Haidian District, Beijing 100083, PR China

[b] Laboratoire de Synthèse, Réactivité Organiques et Catalyse, Institut de Chimie, UMR 7177, Université de Strasbourg, 1 rue Blaise Pascal, 67000 Strasbourg, France

ABSTRACT

This study focuses on the heterogeneous Fenton-like reaction performed over a novel hybrid Cu−Mn−O catalyst for the degradation of a model compound benzophenone-3 (BP-3) in aqueous media. The hybrid Cu−Mn−O catalysts with different Cu/Mn molar ratios were synthesized using co-precipitation and hydrothermal methods, and their composition and morphology were characterized using XRD and SEM analyses. Key parameters including the Cu/Mn ratio in the synthesis, pH and titration of H_2O_2 were shown to significantly influence the degradation of BP-3. A hybrid catalyst with a chemical composition of $Cu_{1.4}Mn_{1.6}O_4$, Mn_3O_4, and Mn_2O_3 exhibiting a morphology of nanofibers and nanoparticles demonstrated the highest catalytic activity in the degradation of BP-3. After 240 min of degradation, 81.5% of BP-3 was removed, which could be mostly related to the presence of hydroxyl radicals ($^{\bullet}$OH). Unlike the conventional Fenton reaction that performs well under highly acidic conditions, BP-3 can be degraded in a wider pH range (2.6−7.1) in the Fenton-like reaction presented herein. Considering the mild conditions used for this Fenton-like system, this novel hybrid catalyst remains promising for wastewater treatment.

© 2016 Académie des sciences. Published by Elsevier Masson SAS. All rights reserved.

1. Introduction

Benzophenone-3 (BP-3) is commonly used in UV filters, which has a great ability to absorb and dissipate UV irradiation. A large panel of personal care products contains BP-3 that protects humans and materials from harmful exposure to UV irradiation [1−3]. With an increasing use of UV filters, BP-3 has been released as an effluent into aquatic environment by the direct discharge from the UV filters

industry and the indirect discharge from municipal wastewater, thus leading to a potential threat to aquatic environment and ecology. It has been detected in rivers, lakes, oceans and even in tap water at concentrations between several ng/L and μg/L [4−9]. Conventional wastewater treatment technologies are usually adapted for the removal of BP-3 [10,11]. Hence, there is a need to remove BP-3 from industrial and municipal wastewater by applying various enhanced technologies. Due to the photo-stability under both UV and artificial solar light, BP-3 cannot be easily degraded by photolysis reactions [6,12]. Although BP-3 can be rapidly oxidized by free chlorine, it is also converted into mono- and di-halogenated by-products as well as several halogenated forms of 3-methoxyphenol,

* Corresponding author.
** Corresponding author.
E-mail addresses: qiang.wang.ox@gmail.com, qiangwang@bjfu.edu.cn (Q. Wang), qifei@bjfu.edu.cn (F. Qi).

resulting in an increase of toxicity [13]. Therefore, it is urgent to find new approaches for the removal of BP-3.

Recently, advanced oxidation processes (AOPs) became promising technologies for the removal of refractory chemicals at an acceptable cost [14]. The hydroxyl radicals (˙OH) generated in AOPs play a key role in the degradation of organic pollutants at a fast reaction rate [15–20]. The Fenton reaction has been proven to be one of the most effective technologies to degrade organic pollutants in wastewater because of its simplicity, low price, availability, and small toxicity of its reagents [21,22]. However, there are some limitations: the use of ferric ions resulted in colored effluents, and the formation of iron sludge. In addition, the Fenton reaction works well only under highly acidic conditions (pH 2–3), which seriously hinders its application and raises the cost [23,24]. In order to overcome the drawbacks of the traditional Fenton reaction, many efforts have been made to develop heterogeneous catalysts free of iron [25–29].

In this study, we report a novel hybrid catalyst containing $Cu_{1.4}Mn_{1.6}O_4$, Mn_2O_3 and Mn_3O_4 as an efficient catalyst for the degradation of BP-3 in a wide pH range (2.6–7.1) in the heterogeneous Fenton-like reaction. The influence of some key parameters including the Cu/Mn molar ratio in the synthesis procedure, initial pH, and titration of H_2O_2 was systematically evaluated. Reactive radicals generated during the reaction were also investigated by using a radical quencher.

2. Experimental section

2.1. Synthesis of samples

The catalyst precursor was synthesized by a traditional co-precipitation method. In brief, a salt solution (100 mL) containing a mixture of $Cu(NO_3)_2 \cdot 3H_2O$ and $Mn(NO_3)_2$ was added dropwise to a Na_2CO_3 aqueous solution (100 mL). The pH of the precipitation solution was controlled at ~10.0 using a NaOH (4 M) solution. The resultant solution was transferred to a Teflon-lined stainless steel autoclave and heated at 150 °C for 18 h. The as-obtained precipitate was filtered and rinsed with deionized water and acetone, followed by drying at 60 °C for 24 h. After careful grinding, the as-prepared samples were calcined at 500 °C for 5 h at a heating rate of 10 °C/min.

2.2. Characterization of samples

X-ray diffraction (XRD) measurements of the catalyst powders were recorded using a Shimadzu XRD-7000 instrument in the reflection mode with Cu Kα radiation. The accelerating voltage was set at 40 kV with 30 mA current ($\lambda = 1.542$ Å) at $0.1°s^{-1}$ from 5 to 65°. Field emission scanning electron microscopy (FE-SEM) and energy-dispersive X-ray spectroscopy (EDX) analyses were performed on an SU-8010 scanning electron microscope (SEM, HITACHI, Japan) with an accelerating voltage of 5.0 kV. Powdered samples were spread on a carbon tape and then coated with a thin platinum layer to prevent charging and improve the image quality.

2.3. Fenton-like reaction procedure

The adsorption or oxidation of BP-3 was carried out in a 300 mL glass reactor containing 250 mL BP-3 solution (2.0 mg/L). In the experiments, certain amounts of catalysts (100 mg/L) and H_2O_2 (0.5–3.0 mM) were added to the BP-3 solution to start the Fenton-like reaction. About 3.0 mL samples were taken out and immediately filtered every 30 min. Before the addition of the catalyst, the initial solution pH was adjusted using nitric acid and/or sodium hydroxide solution. The residual concentration of BP-3 was measured by Waters2695 (Waters, USA) performance liquid chromatography (HPLC) equipped with a UV detector at 288 nm. The separation was performed with an Agilent C18 column (150 mm × 4.6 mm, 5 μm, Agilent, USA) using an isocratic elution of 40% buffered solution ($H_2O/H_3PO_4 = 1000/0.06$, v/v) and 60% CH_3CN. The elution flow rate was 1.0 mL/min and the injection volume was 30 μL for all samples.

3. Results and discussion

3.1. Synthesis and characterization of samples

Fig. 1(a) shows the XRD patterns of samples synthesized with different Cu/Mn molar ratios before calcination. When the quantity of manganese was superior to the loading and the molar ratio of Cu/Mn was 0.05 and 0.2, a hybrid phase of $MnCO_3$ and Mn_3O_4 was obtained. With the Cu/Mn molar ratio increased to 0.5, the Mn_3O_4 phase disappeared and a new $CuMnO_2$ structure was formed. However, the phase of the sample transformed to pure $MnCO_3$ at Cu/Mn = 1.0. By further increasing the ratio of Cu/Mn to 5, the characteristic peaks of CuO were observed at $2\theta = 32.50°$, $35.54°$, $38.70°$, $48.71°$, $58.26°$, and $61.52°$, respectively. Fig. 1(b) shows the XRD patterns of all the samples after calcination at 500 °C for 5 h. With the Cu/Mn ratio of 0.05, the sample was composed of both Mn_2O_3 (JCPDS No. 24-0508) and Mn_5O_8 (JCPDS No. 39-1218). Besides, the diffraction peaks at $2\theta = 35.78°$, $43.96°$, and $63.93°$ might be attributed to Cu_4O_3 (JCPDS No. 49-1830). However, when the ratio of Cu/Mn increased to 0.2, a new hybrid compound of $Cu_{1.4}Mn_{1.6}O_4$, Mn_2O_3 and Mn_3O_4 was obtained. The characteristic reflections of $Cu_{1.4}Mn_{1.6}O_4$ were detected at $2\theta = 18.49°$, $30.42°$, $35.83°$, $57.60°$, and $63.26°$. Furthermore, the diffraction peaks at $2\theta = 28.88°$, $44.44°$, and $64.65°$ might be attributed to Mn_3O_4 (JCPDS No. 24-0734). Further raise in the Cu/Mn molar ratio to 0.5 led to the vanishing of the Mn_2O_3 contribution. When a higher Cu/Mn ratio of 1.0 was used, pure $Cu_{1.5}Mn_{1.5}O_4$ was obtained. As the ratio increased to 5.0, CuO (JCPDS No. 48-1548) emerged in the hybrid sample.

The samples were further characterized by FE-SEM and EDX. Fig. 2 highlights a Cu/Mn ratio increased from 0.05 to 5.0, allowing us to produce all samples in the form of nanoparticles. Surprisingly, nanofibers were also found in the sample synthesized with the Cu/Mn molar ratio as 0.2. Elemental mapping (Fig. 3(b–d)) of Cu, Mn, and O clearly indicated that Cu, Mn, and O were uniformly distributed. This data were also confirmed by the EDX result in certain selected areas in Fig. 4, which demonstrated that the
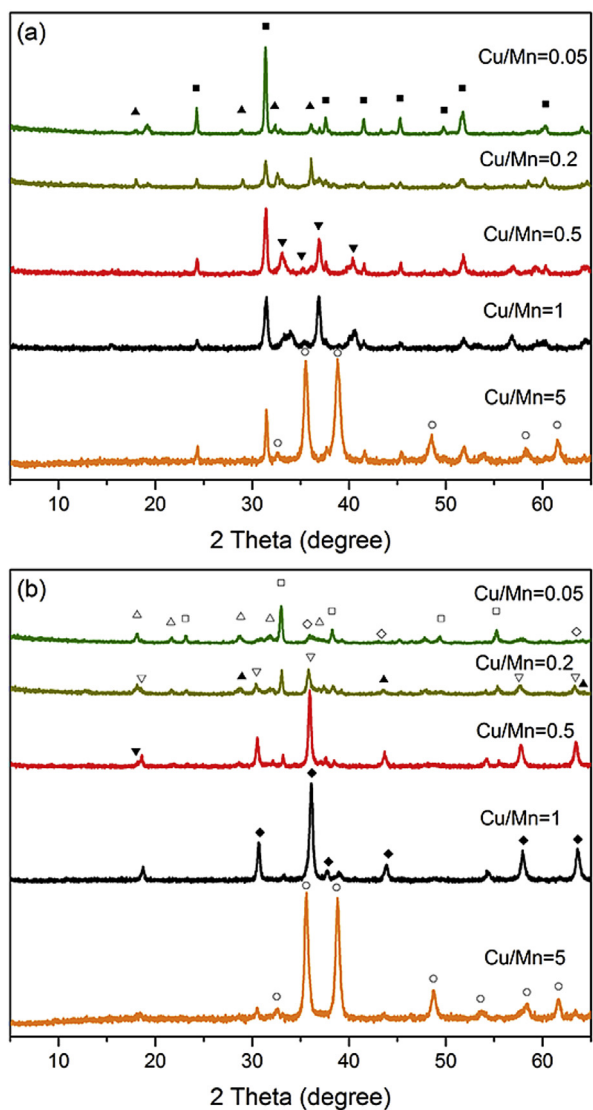
Fig. 1. XRD patterns of samples synthesized with different Cu/Mn ratios. (a) before calcination, (b) after calcination, (■) $MnCO_3$, (▲) Mn_3O_4, (▼) $CuMnO_2$, (○) CuO, (□) Mn_2O_3, (△)Mn_5O_8, (◇) Cu_4O_3, (▽) $Cu_{1.4}Mn_{1.6}O_4$, and (◆) $Cu_{1.5}Mn_{1.5}O_4$.

chemical composition of nanoparticles and nanofibers remained similar. The phase structure and morphology of the as-synthesized samples may have an influence on the performance of the Fenton-like reaction.

3.2. Degradation of BP-3 in the Fenton-like reaction

3.2.1. Influence of the Cu/Mn ratio on BP-3 removal

Since the Cu/Mn molar ratio has a significant effect on the chemical composition and morphology of the samples, further studies were carried out to test their catalytic activities in BP-3 degradation. Without any catalyst addition, the removal of BP-3 was very low, only 39.3% of BP-3 could be decomposed after 240 min. As shown in Fig. 5, the removal efficiency of BP-3 increased while raising the Cu/

Mn ratio at first (before 0.2) and then diminished. When the catalyst was composed of Mn_2O_3, Mn_5O_8 and Cu_4O_3 (Cu/Mn = 0.05), the degradation efficiency of BP-3 reached 73%. Such manganese and copper oxides have been proved to enhance the generation of reactive radicals, which are able to promote the degradation efficiency of pollutants in such reactions [30–32]. The catalyst synthesized with Cu/Mn = 0.2 with a hybrid phase composition of $Cu_{1.4}Mn_{1.6}O_4$, Mn_3O_4, and Mn_2O_3 was observed to exhibit the highest activity, thus leading to a degradation efficiency of 81.5% within 240 min of the reaction. When the Cu/Mn molar ratio was raised to 0.5, the Mn_2O_3 phase disappeared and the oxidation efficiency decreased to 75.0%. With further increasing the molar ratio of Cu/Mn to 1.0 and 5.0, the catalytic activity diminished to 73.3% and 74.6%, respectively, with the phase composition of $Cu_{1.5}Mn_{1.5}O_4$ and CuO. It can be concluded that Mn (III) oxides greatly enhanced the generation of radicals, which play a crucial role in the improvement of the catalytic activity of $Cu-Mn-O_4$. Comparing to manganese oxides, the effect of copper oxides on the improvement of the catalytic activity of $Cu-Mn-O_4$ in the Fenton-like reaction was not significant.

In addition to the effect of the chemical composition, the catalytic activity might also be affected by their particle morphologies. Indeed, all catalysts were observed as nanoparticles except the hybrid catalyst synthesized with Cu/Mn = 0.2, which was constituted of nanoparticles and nanofibers. To clarify how the morphology change influences the catalytic activity, much more work is needed.

3.2.2. Influence of the initial solution pH on BP-3 removal

Since the pH of the solution affects the H_2O_2 decomposition rate, the distribution of BP-3 species, and the surface charge of the catalyst, the effect of the initial solution pH on the performance of BP-3 degradation was investigated. Fig. 6 clearly demonstrates that the highest degradation efficiency of BP-3 was obtained at a pH around 7.1 (81.5% after 240 min). Interestingly, the influence of the initial solution pH (from 2.6 to 7.1) on the final performance and observed degradation rate constant was less than 12.7%. To the best of our knowledge, a traditional Fenton reaction system works well only under highly acidic conditions (pH < 4.0), which was one of the main drawbacks of this reaction system [33]. The catalyst synthesized at Cu/Mn = 0.2 showed high catalytic activity at a wide pH range, which made the successful application of this effective Fenton-like reaction for a real wastewater treatment.

Moreover, the oxidation of BP-3 with different initial solution pH can be fitted by pseudo–first-order kinetics model described by the following equations (Eqs. 1–4), as $[H_2O_2] \gg [BP\text{-}3]$ in this study.

$$-\frac{d[BP-3]}{dt} = k[H_2O_2][BP-3] \tag{1}$$

$$k_{obs} = k[H_2O_2] \tag{2}$$
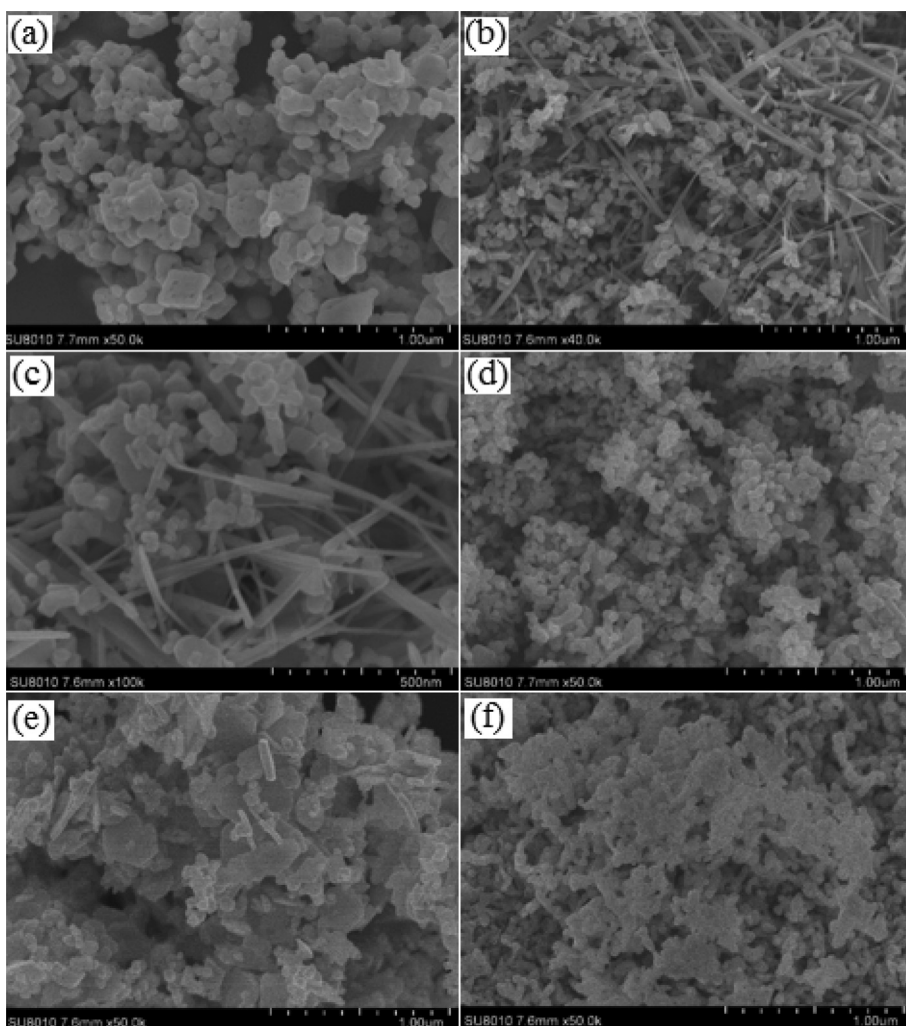
Fig. 2. SEM images of samples synthesized with different Cu/Mn ratios (calcined at 500 °C for 5 h). (a) Cu/Mn = 0.05, (b) Cu/Mn = 0.2, (c) the high-resolution SEM of Cu/Mn = 0.2, (d) Cu/Mn = 0.5, (e) Cu/Mn = 1.0, and (f) Cu/Mn = 5.0.

$$-\frac{\mathrm{d}[BP-3]}{\mathrm{d}t} = k_{\mathrm{obs}}[BP-3] \qquad (3)$$

$$\ln\left(\frac{[BP-3]}{[BP-3]_0}\right) = k_{\mathrm{obs}}t \qquad (4)$$

where k_{obs} is the pseudo-first-order rate constant and [BP−3] is the concentration of BP−3 at reaction time t. The k_{obs} value can be obtained by linear regression of the plot of ln ([BP−3]$_t$/[BP−3]$_0$) versus t. The influence of the initial solution pH on the value of k_{obs} is shown in Fig. 7. Under acidic conditions (pH < 3.0), a fast degradation rate was observed due to the dissolution of copper and manganese from the solid catalyst. The homogeneous Fenton reaction will lead to a fast reaction. From pH = 3.4 to 7.1, the reaction change from a homogeneous reaction to a heterogeneous one, thus resulting in a lower reaction rate. Indeed, limited mass transfer can be expected in the latter case. The BP-3

species will change according to water pH variation, as shown in the inset of Fig. 7. The increase of BP-3⁻ species would lead to stronger electrostatic attraction on the surface of Cu−Mn−O, resulting in a higher reaction rate from water pH = 3.4 to 7.1. However, when the pH was over 7.1, the reaction rate started to decrease. This might be because the surface adsorption caused by electrostatic attraction was decreased due to the surface negative charge of Cu−Mn−O.

3.2.3. Influence of the H$_2$O$_2$ quantity on BP-3 removal

In order to test the role of surface adsorption in this Fenton-like reaction, a pre-adsorption experiment was designed and carried out as well (Fig. 8). Only the catalyst with Cu/Mn = 0.2 was added in the first 30 min, and the adsorption efficiency was only 7.9% after 30 min. The pK_a value of BP-3 is 9.57 [34], leading to the formation of BP-3⁻ and BP-3 species under water pH = 7.0. The presence of BP-3⁻ will lead to a surface adsorption on Cu−Mn−O by electrostatic attraction. The catalytic oxidation process can
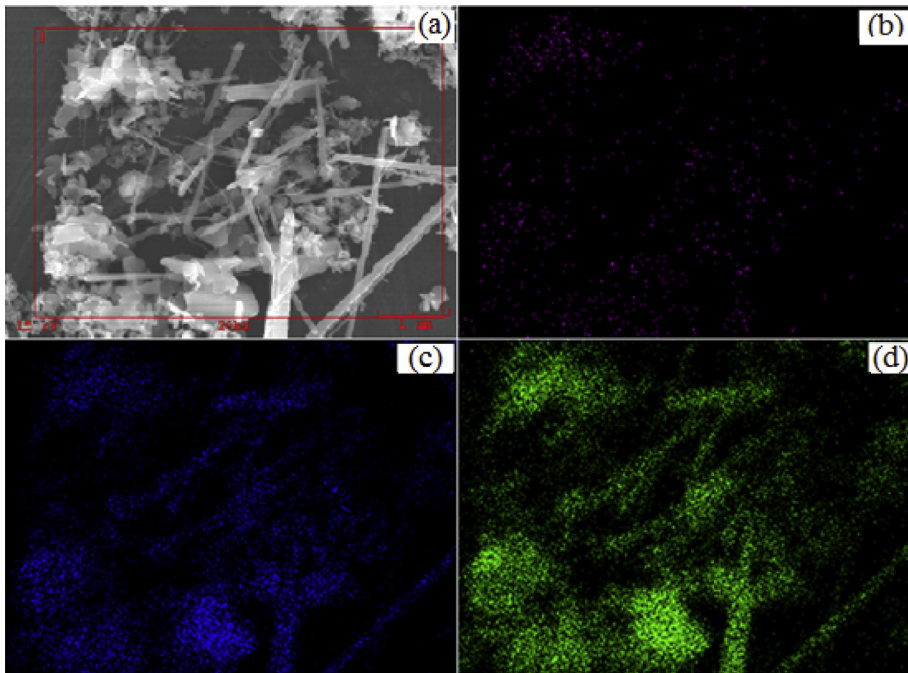
Fig. 3. (a) SEM image of sample synthesized with a Cu/Mn molar ratio of 0.2. Elemental (b) Cu mapping, (c) Mn mapping, and (d) O mapping of the synthesized sample.

be observed by adding H_2O_2 to the reaction system. The degradation efficiency significantly increased to 89.0% after 240 min. This experiment clearly indicated that BP-3 adsorption on the catalyst was not obvious and its significant degradation came from the catalytic oxidation in the presence of H_2O_2. Moreover, at the beginning 150 min of H_2O_2 addition, the catalyst exhibited less catalytic activity for BP-3 removal, compared with the process without pre-adsorption. This phenomenon can be explained by the fact that BP-3 is firstly absorbed on the catalyst surface, which
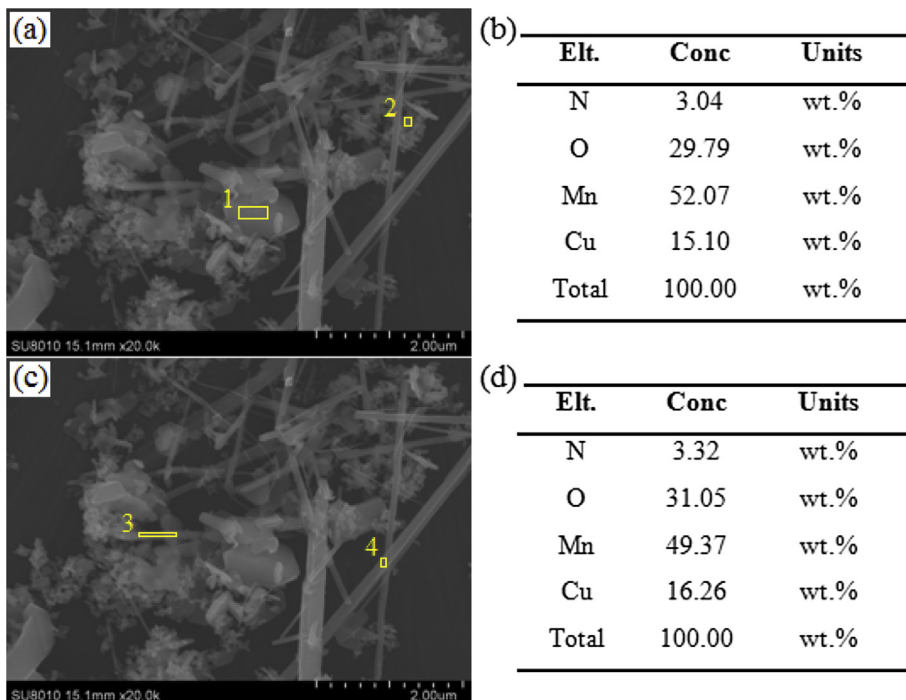

Fig. 4. SEM-EDX analysis of the sample synthesized at Cu/Mn = 0.2. (a, b) Nanoparticles and (c, d) nanofibers.
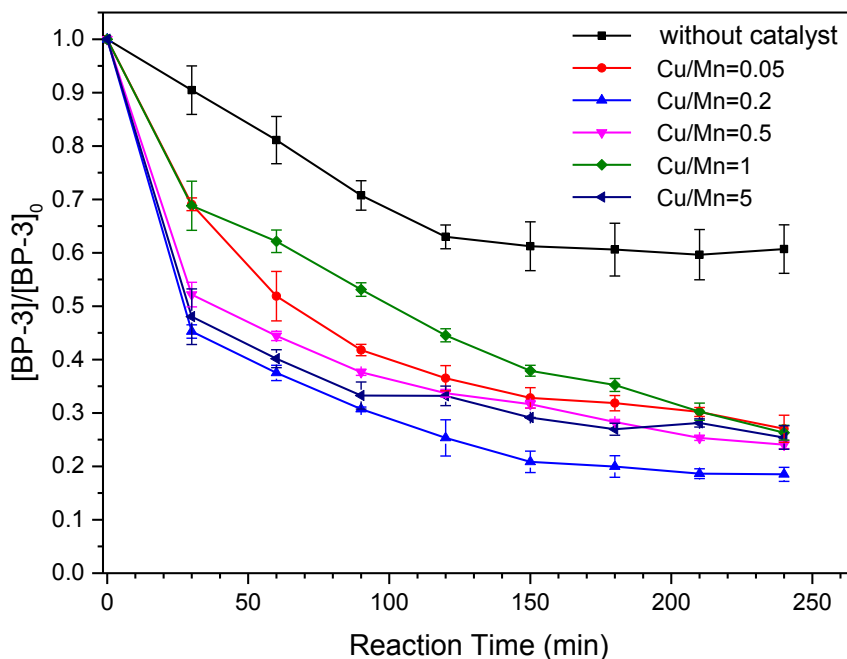
Fig. 5. The influence of different molar ratios of Cu/Mn on the degradation of BP-3 in the Fenton-like reaction. Reaction conditions: $[BP\text{-}3]_0 = 2.0$ mg/L, $[H_2O_2]_0 = 1.0$ mM, $[catalyst]_0 = 100$ mg/L, and pH = 7.0.

affected the mass transfer of H_2O_2 and hindered the Fenton-like reaction. As the oxidation proceeded, the surface adsorbed BP-3 was degraded, and dissolved BP-3 would be gradually adsorbed and then degraded by the Fenton reaction.

The influence of the H_2O_2 concentration on the degradation of BP-3 was also investigated. The experimental results revealed a faster and higher BP-3 removal at higher H_2O_2 concentrations. The pseudo-first-order rate constant (k_{obs}) showed a linear relationship with H_2O_2
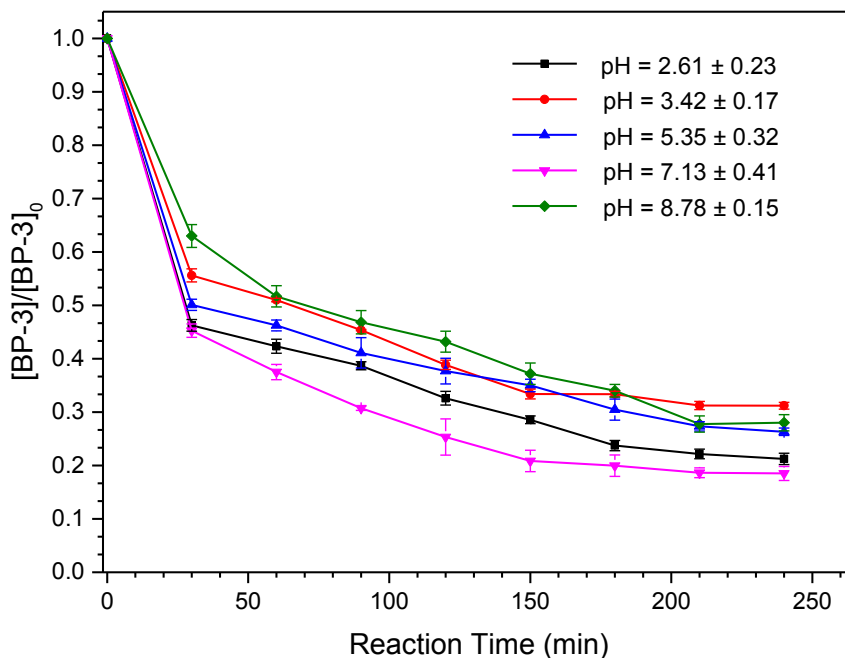
Fig. 6. The influence of the initial solution pH on the degradation BP-3 by the sample synthesized at Cu/Mn = 0.2. Reaction conditions: $[BP\text{-}3]_0 = 2.0$ mg/L, $[H_2O_2]_0 = 1.0$ mM, $[catalyst]_0 = 100$ mg/L, and the initial solution pH was adjusted by HNO_3 and NaOH.
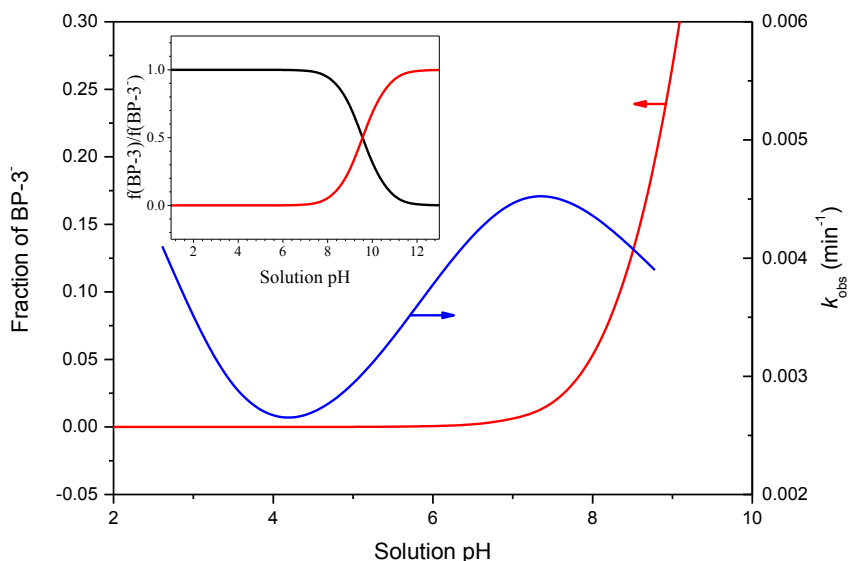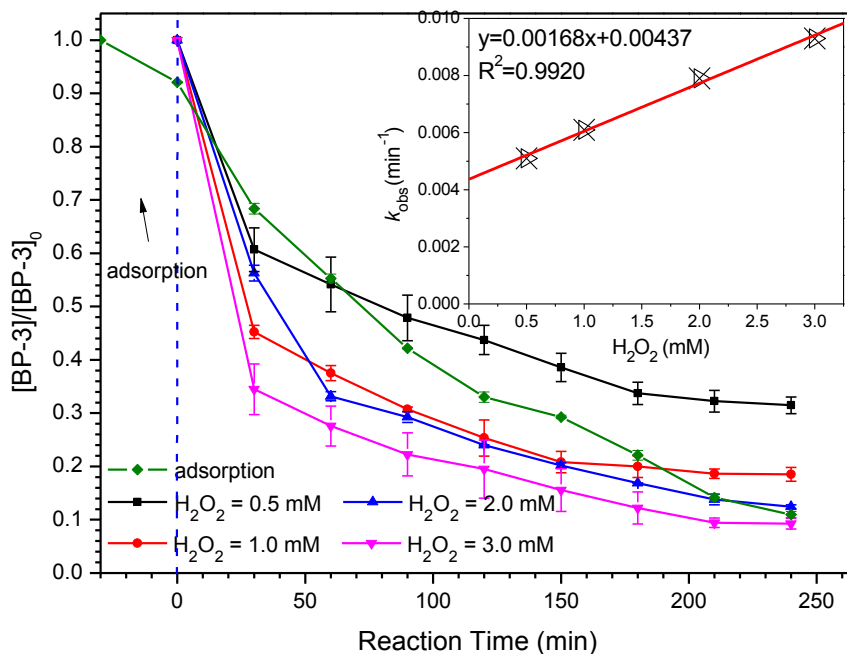
Fig. 7. Variation of the pseudo-first-order rate constant as a function of the initial solution pH for BP-3 degradation. Reaction conditions: $[BP-3]_0 = 2.0$ mg/L, $[H_2O_2]_0 = 1.0$ mM, and $[catalyst]_0 = 100$ mg/L.

concentrations (inset of Fig. 8), which can be attributed to more reactive radicals generated from H_2O_2 in the aqueous medium. The results of over dosing H_2O_2 or ·OH quenching by H_2O_2 were not obtained in this study.

3.2.4. Influence of the hydroxyl free radical on BP-3 removal

In order to better understand the role of ·OH in BP-3 degradation, *tert*-butanol (TBA) that can quench ·OH [35] was added into the reaction system. According to Fig. 9,

when the TBA dose was 50 mg/L, the removal rate decreased to 71.5%, suggesting that the presence of ·OH accounted for the oxidation of BP-3. By further increasing the concentration of TBA to 250 mg/L, the trend of BP-3 concentration variation was not significantly modified, indicating that the dose of TBA quenched all ·OH generated in this Fenton-like reaction. Hence, ·OH produced in the Fenton-like reaction might play a crucial role in the catalytic oxidation of BP-3.

Fig. 8. The influence of pre-adsorption and different initial H_2O_2 concentrations on the degradation of BP-3 by the sample synthesized at Cu/Mn = 0.2. The inset shows the variation of the pseudo-first-order rate constant as a function of the H_2O_2 concentration for BP-3 degradation. Reaction conditions: $[BP-3]_0 = 2.0$ mg/L, $[catalyst]_0 = 100$ mg/L, and pH = 7.0.
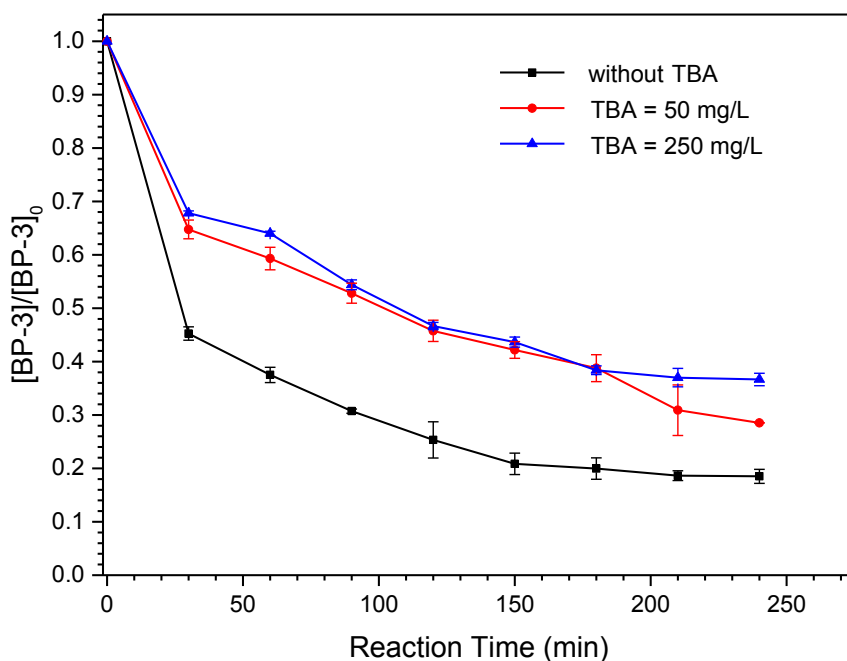
Fig. 9. The influence of TBA on the degradation BP-3 by the sample synthesized at Cu/Mn = 0.2. Reaction conditions: $[BP-3]_0 = 2.0$ mg/L, $[H_2O_2]_0 = 1.0$ mM, $[catalyst]_0 = 100$ mg/L, and pH = 7.0.

4. Conclusions

In conclusion, a novel hybrid Cu–Mn–O catalyst was synthesized using a co-precipitation and hydrothermal method, which showed high catalytic activity on the degradation of BP-3 in the heterogeneous Fenton-like reaction. XRD and SEM analyses suggest that this hybrid Cu–Mn–O catalyst (Cu/Mn = 0.2) consists of $Cu_{1.4}Mn_{1.6}O_4$, Mn_3O_4, and Mn_2O_3, with a morphology containing both nanoparticles and nanofibers. The catalytic activity, the chemical composition, and the morphology of catalyst were highly dependent on the Cu/Mn ratio in the synthesis. The influence of the solution pH on the final performance and the observed degradation rate constant was less than 12.7%, suggesting that the heterogeneous Fenton-like reaction with this novel hybrid Cu–Mn–O catalyst was less sensitive to solution pH values. Since this hybrid Cu–Mn–O catalyst is applicable in a much wider pH range (2.6–7.1) than conventional Fenton systems, it is very promising for practical wastewater treatment systems. The dose of H_2O_2 was demonstrated to be good for raising the removal efficiency of BP-3, and the reaction was verified to be dominated by ·OH radicals.

Acknowledgements

References

[1] J. Krutmann, Prog. Biophys. Mol. Biol. 92 (2006) 105.

[2] U. Hauri, B. Lütolf, C. Hohl, Mitt. Leb. Hyg. 94 (2003) 80.
[3] V. Bissonauth, R. Drouin, D.L. Mitchell, M. Rhainds, J. Claveau, M. Rouabhia, Clin. Cancer Res. 6 (2000) 4128.
[4] P. Kunz, H. Galicia, K. Fent, Toxicol. Sci. 90 (2006) 349.
[5] N. Bluthgen, S. Zucchi, K. Fent, Toxicol. Appl. Pharmacol. 263 (2012) 184.
[6] R. Rodil, M. Moeder, R. Altenburger, M. Schmitt-Jansen, Anal. Bioanal. Chem. 395 (2009) 1513.
[7] M. Schlumpf, B. Cotton, M. Conscience, V. Haller, B. Steinmann, W. Lichtensteiger, Environ. Health Perspect. 109 (2001) 239.
[8] M.E. Balmer, H.R. Buser, M.D. Müller, T. Poiger, Environ. Sci. Technol. 39 (2005) 953.
[9] S. Díaz-Cruz, M. Gago-Ferrero, M.P. Llorca, D. Barceló, Anal. Bioanal. Chem. 402 (2012) 2325.
[10] W. Li, Y. Ma, C. Guo, W. Hu, K. Liu, Y. Wang, T. Zhu, Water Res. 41 (2007) 3506.
[11] N. Negreira, I. Rodríguez, M. Ramil, E. Rubi, R. Cela, Anal. Chim. Acta 654 (2009) 162.
[12] Y.S. Liu, G.G. Ying, A. Shareef, R.S. Kookana, Environ. Chem. 8 (2011) 581.
[13] N. Negreira, P. Canosa, I. Rodriguez, M. Ramil, E. Rubi, R. Cela, J. Chromatogr. A 1178 (2008) 206.
[14] A.H. Joss, H. Siegrist, T.A. Ternes, Water Sci. Technol. 57 (2008) 251.
[15] H. Liu, C. Wang, X.Z. Li, X.L. Xuan, C.C. Jiang, H.N. Cui, Environ. Sci. Technol. 41 (2007) 2937.
[16] Y. Du, M. Zhou, L. Lei, Water Res. 41 (2007) 1121.
[17] J. Sun, S. Sun, G. Wang, L. Qiao, Dyes Pigments 74 (2007) 647.
[18] Z. Zhang, R. Yang, Y. Gao, Y. Zhao, J. Wang, L. Huang, J. Guo, T. Zhou, P. Lu, Z. Guo, Q. Wang, Sci. Rep. 4 (2014) 6797.
[19] Y. Zhang, Z. Zhang, Q. Yan, Q. Wang, Appl. Catal. A-Gen 511 (2016) 47.
[20] Z. Zhang, F. Xu, Y. Zhang, A. Umar, Q. Wang, Catal. Today (2016), http://dx.doi.org/10.1016/j.cattod.2015.10.031.
[21] L.I. Doumic, P.M. Haure, M.C. Cassanello, M.A. Ayude, App. Catal. B-Environ. 142–143 (2013) 214.
[22] G.K. Zhang, Y.Y. Gao, Y.L. Zhang, Y.D. Guo, Environ. Sci. Technol. 44 (2010) 6384.
[23] A. Ventura, G. Jacquet, A. Bermond, V. Camel, Water Res. 36 (2002) 3517.
[24] Z.H. Ai, L.R. Lu, J.P. Li, L.Z. Zhang, J.R. Qiu, M.H. Wu, J. Phys. Chem. C 111 (2007) 7430.
[25] J.G. Yu, X.X. Yu, B.B. Huang, X.Y. Zhang, Y. Dai, Cryst. Growth Des. 9 (2009) 1474.
[26] M.M. Cheng, W.J. Song, W.H. Ma, C.C. Chen, J.C. Zhao, J. Lin, H.Y. Zhu, Appl. Catal. B 77 (2008) 355.

[27] A.L.-T. Pham, C.H. Lee, F.M. Doyle, D.L. Sedlak, Environ. Sci. Technol. 43 (2009) 8930.
[28] J.H. Ramirez, F.J. Maldonado-Hódar, A.F. Pérez-Cadenas, C. Moreno-Castilla, C.A. Costa, L.M. Madeira, Appl. Catal. B 75 (2007) 312.
[29] M.B. Kasiri, H. Aleboyeh, A. Aleboyeh, Appl. Catal. B 84 (2008) 9.
[30] S. Jauhar, M. Dhiman, S. Bansal, S. Singhal, J. Sol-Gel Sci. Technol. 75 (2015) 124.
[31] M. Das, K.G. Bhattacharyya, Chem. Eng. Commun. 202 (2015) 1657.
[32] L. Lyu, L. Zhang, C. Hu, Chem. Eng. J. 274 (2015) 298.
[33] J.H. Ma, W.H. Ma, W.J. Song, C.C. Chen, Y.L. Tang, J.C. Zhao, Environ. Sci. Technol. 40 (2006) 618.
[34] B. Yang, G.G. Ying, Water Res. 47 (2013) 2458.
[35] J. Staehelin, J. Hoigne, Environ. Sci. Technol. 19 (1985) 1206.